Int J Hum Genet, 20(4): 179-190 (2020)
PRINT: ISSN 0972-3757 ONLINE: ISSN 2456-6330
DOI: 10.31901/24566330.2020/20.04.764

FGF3-Related Phenotypes: A Study of LAMM Syndrome and Otodental Dysplasia Patients with Two Novel Mutations in *FGF3* Gene

Ayberk Turkyilmaz[1], Bilgen Bilge Geckinli[2], Ceren Alavanda[2], Gülçin Zengin[3], Esra Arslan Ates[4] and Ahmet Arman[2]

[1]Department of Medical Genetics, Erzurum City Hospital, Erzurum, Turkey
[2]Department of Medical Genetics, School of Medicine, Marmara University, Istanbul, Turkey
[3]Department of Radiology, School of Medicine, Marmara University, Istanbul, Turkey
[4]Department of Medical Genetics, Marmara University Pendik Training and Research Hospital, Istanbul, Turkey

KEYWORDS *FGF3* Gene. Michel's Aplasia. Novel Variant. Sensorineural Hearing Loss. Splice-Site Variant

ABSTRACT The fibroblast growth factor (FGF) signaling pathway regulates the intracellular events which are involved in the proper formation of the internal organs and limbs during the earliest stages of embryonic development. Here, the researchers performed a detailed examination of clinical and radiological findings from syndromic cases with sensorineural hearing loss and determined their molecular genetic etiology. Family history, physical examination, laboratory and radiological examinations for three Turkish families displaying congenital sensorineural hearing loss, microtia, dental anomalies and neuromotor developmental delay were evaluated and molecular analysis of the *FGF3* gene was performed. The researchers detected a heterozygous deletion of a 2.4 Megabase (Mb) segment in the region spanning 68,734,891 to 71,538,481 bases in the chromosome 11q13.3-q13.4. Interestingly, this region included the *FGF3* gene in case 1, whereas two novel mutations (NM_005247: c.8T>G, p.Leu3Arg, NM_005247: c.324+2T>C) were identified in case 2 and case 3 respectively. From this study, the researchers conclude that in the absence of inner ear structures in cases of syndromic hearing loss, *FGF3* gene related phenotypes should be considered and the *FGF3* gene should be examined by sequence analysis and array-CGH methods for both point mutations and gross deletions.

INTRODUCTION

The fibroblast growth factor 3 (*FGF3*) gene comprises of 3 exons located on the chromosome 11q13.3 and encode a 239 amino acid protein. The resulting protein, known as the fibroblast growth factor (FGF), regulates several signal pathways which are involved in the proper formation of the inner ear structures via specific intracellular events during the embryonic development (Ornitz et al. 2001; Alvarez et al. 2003; Wright et al. 2003). Defects in the FGF signaling pathway can lead to disruption in cochlear coiling as well as formation of endolymphatic duct and semicircular canals (Mansour et al. 1993; Pauley et al. 2003; Hatch et al. 2007). Mutations in the *FGF3* and *FGF10* genes can therefore cause disruptions in the signal pathway which can lead to diseases associated with defects of the inner ear structures (Rohmann et al. 2006; Tekin et al. 2007). A study by Gregory-Evans et al. (2007) found that microdeletions at the 11q13 region of the chromosome, which also contains the *FGF3* gene, causes otodental syndrome (Gregory-Evans et al. 2007). Moreover, they found that anomalies of the inner ear development occurred in addition to tooth and eye manifestations, which are the main symptoms of the syndrome. Subsequently, the LAMM syndrome phenotype was defined by Tekin et al. (2008) and these patients displayed facial dysmorphism, congenital sensorineural hearing loss, microtia, microdontia and neuromotor developmental retardation (Tekin et al. 2008; Al Yassin et al. 2019; Basdemirci et al. 2019).

Address for correspondence:
Ayberk Turkyilmaz, MD,
Department of Medical Genetics,
Erzurum City Hospital,
Ataturk Quarter, Cat Yolu Street,
25070 Yakutiye, Erzurum, Turkey
Telephone: +905058120334,
Fax: +904422327383,
E-mail: ayberkturkyilmaz@gmail.com

Recent studies have shown that variants of the *FGF3* gene can be associated with temporomandibular joint disease, rotator cuff disease as well as tooth agenesis (Küchler et al. 2013; Motta et al. 2014; Carpio et al. 2019; Cunha et al. 2020). In addition, a relationship between the FGF3-BMP signaling pathway and neural tube closure, neural crest specification, and axis termination has been described (Anderson et al. 2016). Interestingly, *FGF3* gene copy number variations and point mutations have also been associated with different types of cancers such as that of the breast, prostate, esophagus, and oral squamous cell carcinoma (Li et al. 2015; Chung et al. 2019; Anwar et al. 2020; Brown et al. 2020).

Till date, a total of 24 mutations have been identified in the *FGF3* gene, of which approximately half (54%) were missense/nonsense mutations. Further, 17 percent of mutations were small deletions leading to frameshift, 4 percent were small indels leading to frameshift, 12.5 percent were gross deletions and 2.5 percent were gross insertions. From this, it has been concluded that all heterozygous gross deletions including those in the *FGF3* gene are associated with otodental dysplasia whereas homozygous / compound heterozygous single nucleotide variations are associated with LAMM syndrome phenotype (https: //portal.biobase-international. com/hgmd/pro/all.php).

In this study, family history, physical examination, laboratory, and radiological examinations for three different Turkish families with congenital sensorineural hearing loss, microtia, dental anomalies and neuromotor developmental delay were evaluated and molecular analysis of *FGF3* gene was performed.

Objective

In this study, the researchers aimed to perform a detailed examination of the clinical and radiological findings of syndromic cases which display sensorineural hearing loss and to determine their molecular genetic etiology. They focused on the examination of the *FGF3* gene using different molecular methods, especially in syndromic cases with sensorineural hearing loss with an absence of inner ear structures.

METHODOLOGY

All experimental procedures were conducted in accordance with the principles of the Declaration of Helsinki and were approved by the Local Ethical Committee. Informed written consent was obtained from parents of test subjects included in this study. Three cases from three different families were evaluated and their selection was based on family history, physical examination, laboratory and radiological examinations. *FGF3* gene associated LAMM syndrome and otodental dysplasia phenotypes were considered as primary diagnosis and then molecular genetic analysis of these cases were performed as described below.

First, genomic DNA was isolated using the QiaAmpDNA Mini kit (QIAGEN Germantown, MD, USA) from peripheral blood leukocytes of index cases. All exons and exon–intron junctions of the *FGF3* gene for patients were amplified by polymerase chain reaction (PCR) using custom designed primers (Primer sequences: exon 1 forward primer: 5'-CACCTTTCCCGCGAAGCCG-3'; exon 1 reverse primer: 5'-CGCACCATGCCT-TCTCCCG-3'; exon 2 forward primer: 5'-CTTC-CACTCACTCCCCGACC-3'; exon 2 reverse primer: 5'-GCAAAGCATTCTACTGCCCACATC-3'; exon 3 forward primer: 5'-TGACGCTGCCA-CAGTCTCC-3'; exon 3 reverse primer: 5'-GCTG-GCTCTGGAAATAGCTGAG-3'). The PCR products were sequenced using the Sanger sequence analysis method using the ABI PRISM® 3130xl genetic analyzer (Applied Biosystems, Foster City, CA, USA). To evaluate the pathogenicity of the detected variants, the frequency of the variant in population studies (1000G, ExAC, gnomAD), predictions of in-silico analysis and American College of Medical Genetics and Genomics (ACMG) were used as selection criteria (Richards et al. 2015). Array comparative genomic hybridization (Array-CGH) was performed in case 1 for the otodental dysplasia. Chromosomal microarray analysis was performed on the Affymetrix Cytoscan Optima (315K) chips (Thermo Fisher Scientific, Waltham, MA, USA) using DNA obtained from peripheral blood. The data obtained from the Chromosome Analysis Suite (v3.2.0; Thermo Fisher Scientific, USA) were evaluated using current databases such as Pubmed, Database of Genomic Variants, and DECIPHER.

RESULTS

Clinical Characteristics

Case 1

A 10-month-old male patient was referred to the researchers' clinic for displaying bilateral sensorineural hearing loss and facial dysmorphism. He was born at term by spontaneous vaginal delivery (birth weight: 2850 g [-1.23 standart deviation score (SDS)] and birth height: 48 cm [-0.91 SDS]) and was the first child of non-consanguineous healthy parents. Upon detection of hearing loss in the left ear during newborn hearing screening, the patient underwent the auditory brainstem response (ABR) test for a thorough screening. While ABR results revealed syndromic hearing loss resulting from mild sensorineural hearing loss in the right ear, the researchers detected very advanced sensorineural hearing loss in the left ear as well as facial dysmorphism. Furthermore, patient's height, weight and head circumference measurements were 70 cm (-1.4 SDS), 8000 gr (-1.42 SDS) and 44.5 cm (-1.18 SDS), respectively. Dysmorphological examination revealed a prominent metopic suture, bilateral preauricular skin tags, prominent forehead, long face, small ears, narrow palpebral fissures, narrow and high arched palate and simian crease on the left hand (Fig. 1a-b). Eye examination was normal in the neonatal period; however, head control was delayed and the age of sitting without support was at the 9th month. Organomegaly was not detected in the whole abdomen ultrasonography (USG) of the patient but there was a small atrial septal defect (ASD) detected in the echocardiographic (ECHO) evaluation. Internal acoustic canal (IAC) magnetic resonance imaging (MRI) and temporal bone computed tomography (CT) was conducted owing to asymmetric bilateral sensorineural hearing loss. These tests revealed advanced hypoplasia in the left IAC and the 7th–8th nerve complexes extending into the canal had abnormal appearance. The 7th–8th nerve complex derived from the brainstem in the form of two separate anatomical structures was identified as a uniform single nerve at the entrance of the canal, which extended into the canal (Fig. 2a-b). A physical examination at 2 years of age revealed that the patient's height was 82 cm. (-1.6 SDS), weight was 9500 g. (-2.47 SDS) and head circumference was 47 cm (-1.5 SDS). Upon further phys-

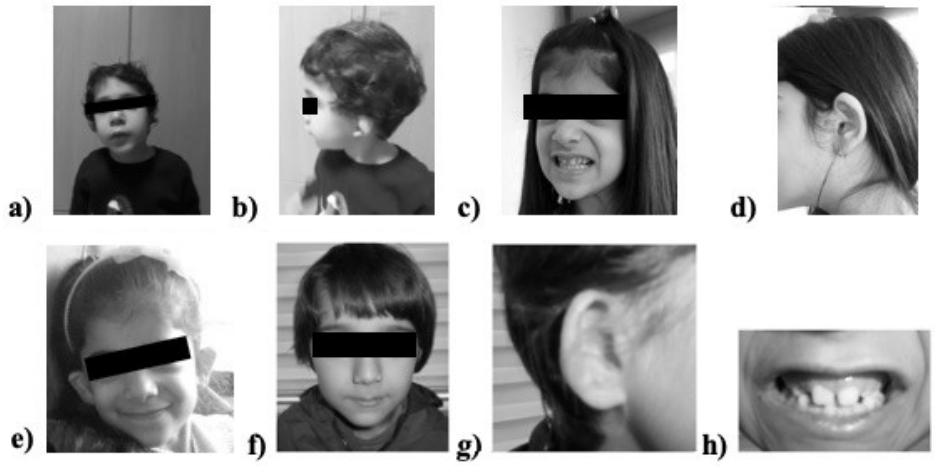

Fig. 1. Dysmorphologic findings of Case 1 a) prominent metopic suture, prominent forehead, long face, narrow palpebral fissures, mild downslanting palpebral fissures; b) bilateral preauricular skin tag, small, low-set and cup-shaped ears. Dysmorphologic findings of case 2; c) long face, deep set eyes, downslanting palpebral fissures, depressed nasal bridge and upturned nasal tip, microdontia, widely spaced teeth; d) preauricular skin tag; e) cupped shaped ears, short philtrum. Dysmorphologic findings of Case 3 f) narrow forehead, long face; g) bilateral postauricular skin tag, small cupped shaped ears; h) microdontia, widely spaced teeth.

ical examination, the researchers observed low-set and cupped shaped small ears, small, and spaced teeth, flat nasal bridge, upturned nasal tip and flat philtrum. At this age, the patient had started to walk and speak a few words but was unable to form a sentence. Due to small ASD, follow-up examination was conducted and eye examination provided normal results. Karyotype, Array-CGH, and *FGF3* gene sequence analysis were performed on the basis of the preliminary clinical and radiological diagnosis revealed otodental dysplasia.

Case 2

A 5-year-old girl was referred to the researchers' clinic for bilateral sensorineural hearing loss and facial dysmorphism. She was born at term by normal vaginal delivery (birth weight: 3040 g [-0.62 SDS]) and was the first child of consanguineous (second cousins) healthy parents. A brainstem implant was placed due to congenital hearing loss. The height, weight and head circumference were measured at 113 cm (+ 0.85 SDS), 17 kg (-0.57 SDS) and 50 cm (-0.48 SDS), respectively. Dysmorphological examination showed narrow forehead, long face, deep set eyes, downslanting palpebral fissures, depressed nasal bridge and upturned nasal tip, small cupped shaped ears, microdontia, widely spaced teeth, short philtrum and preauricular skin tag (Fig. 1c-e). Furthermore, eye examination revealed 2 degrees of myopia, neuromotor evaluation revealed a delayed head control and the age of sitting without support was found to be 10 months. She could walk at 1.5 years of age and could speak a few words at about 3.5 years of age. Her ECHO and whole abdomen USG were normal. ICA MRI evaluation revealed an absence of bilateral inner ear structures, and intracranial segments of the 7th and 8th right nerve and the 7th left cranial nerve were not observed whereas the 8th left cranial nerve was in fine calibration. These pathological observations were consistent with Michel's aplasia (Fig. 2d). The absence of bilateral inner ear structures was also observed in the temporal bone CT evaluation (Fig. 2c). Karyotype and *FGF3* gene sequence analysis were performed on the basis of preliminary diagnosis of LAMM syndrome due to clinical and radiological findings.

Case 3

A 6-year-old male patient was referred to the researchers' clinic for bilateral sensorineural hearing loss and facial dysmorphism. He was born at term by normal vaginal delivery (birth weight: 3950 g [+1.24 SDS]) and was the first child of consanguineous (first cousins) healthy parents. A brainstem implant was placed owing to congenital hearing loss. The height, weight, and head circumference measurements were found to be 124.5 cm (+1.76 SDS), 24 kg (+1 SDS), and 52 cm (+0.14 SDS), respectively. Dysmorphological examination revealed narrow forehead, long face, small cupped shaped ears, microdontia, widely spaced teeth, and bilateral postauricular skin tags (Fig. 1f-h). Results of the eye and heart examination were normal. However a neuromotor evaluation showed delayed head control. The age of sitting without support was 1 year and at 1.5 year of age he could walk. ICA MRI and temporal bone CT examination revealed that bilateral internal acoustic canals, cochlea, vestibule and semicircular canals and the 8th cranial nerves were not observed (Fig. 2e-f). Karyotype and *FGF3* gene sequence analysis were performed considering the preliminary diagnosis of LAMM syndrome owing to the clinical and radiological findings.

Molecular Analysis Results for Patients

The case 1 patient displayed a normal XY male karyotype with 46 chromosomes. Heterozygous deletion of a 2.40 Mb segment in the region spanning from 68,734,891 to 71,538,481 bases on the chromosome section 11q13.3-q13.4 was detected (Fig. 3). Interestingly, the array-CGH examination of the parents yielded normal results which indicates that the mutation was *de novo*. Furthermore, the non-deleted allele of the *FGF3* gene in the case 1 patient was sequenced by Sanger method and no mutation was detected.

Cases 2 and 3 also showed normal 46, XX female and 46,XY male karyotypes, respectively with 46 chromosomes. In the case 2 patient, a novel homozygous missense variant (NM_005247: c.8T>G, p.Leu3Arg) was detected (Fig. 4c). This variant has not been reported in any previous literature in previous population stud-

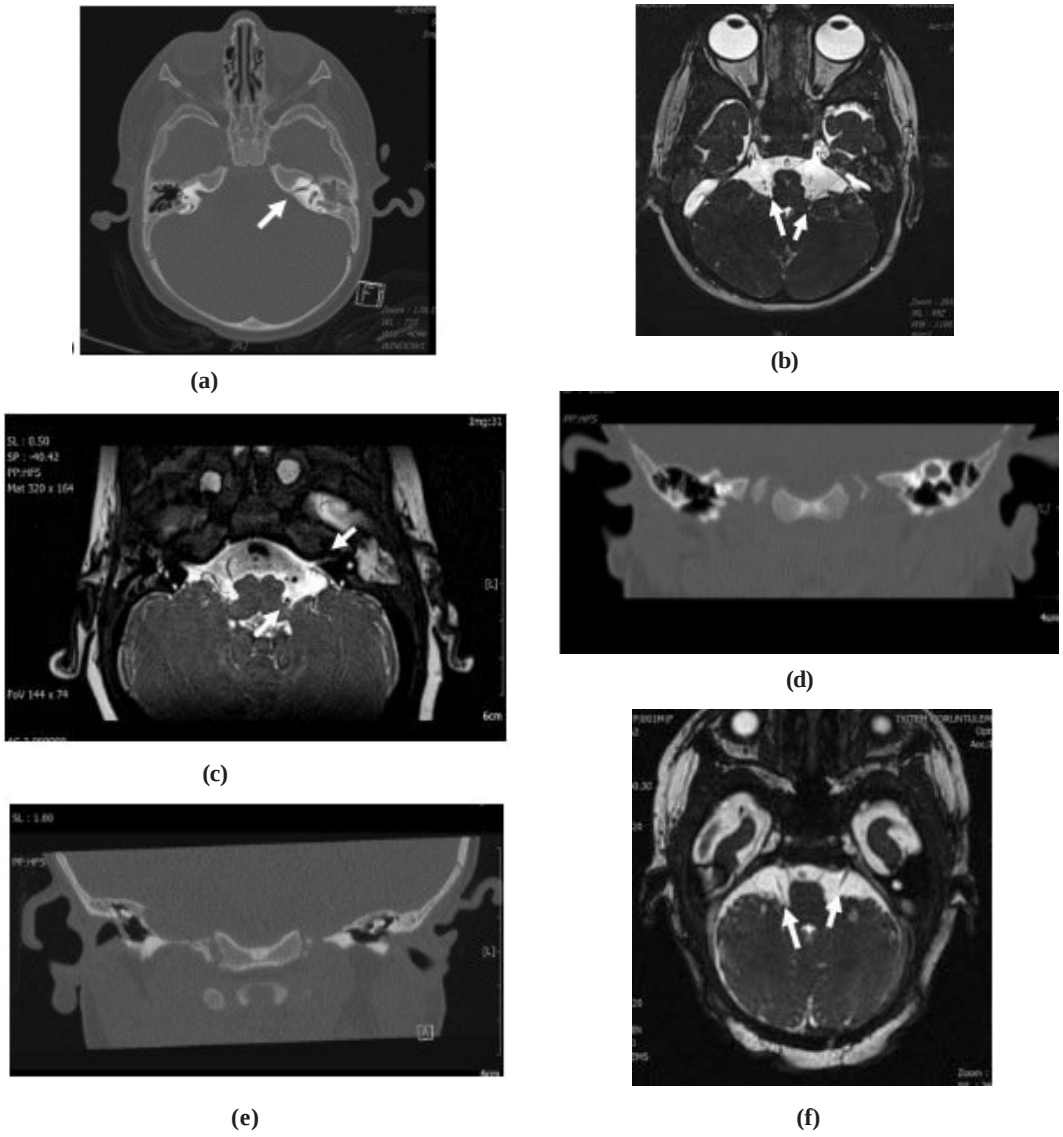

Fig. 2. a) Advanced hypoplasia was demonstrated in the left internal acoustic canal in temporal bone CT of case 1; b) The hypoplastic left 7th–8th nerve complex derived from the brainstem in the form of two separate anatomical structures showed a uniform single nerve at the entrance of the canal, which extended into the canal in this form in ICA MRI of case 1; c) The absence of bilateral inner ear structures was observed in the Temporal Bone CT evaluation of case 2; d) In the ICA MRI evaluation of the case 2, bilateral inner ear structures, intracranial segments of the 7th and 8th right nerve and 7th left cranial nerve were not observed; 8th left nerve was in fine calibration and the current pathology was consistent with Michel's aplasia; e) Temporal bone CT examination of the case 3 revealed that bilateral cochlea, vestibule and semicircular canals were not observed (complete labyrinthine aplasia); f) In the ICA MRI evaluation of the case 3, bilateral aplasia of the 8th nerves and intracranial segments of the 7th nerves were detected.

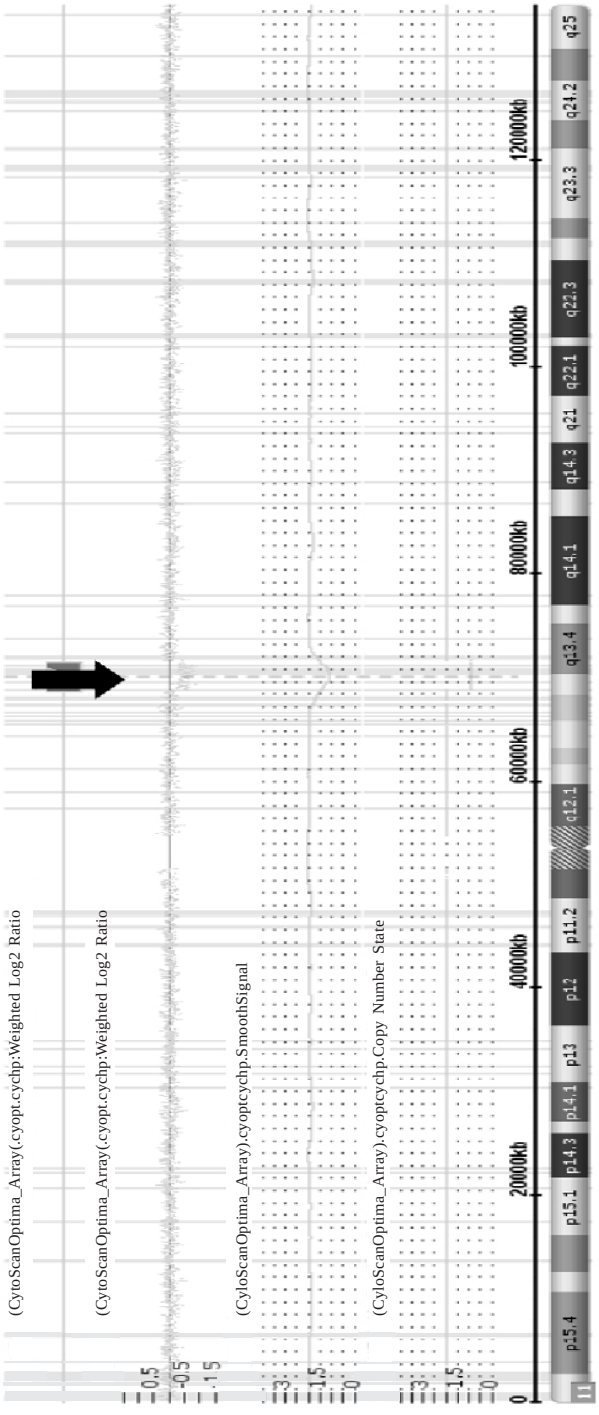

Fig. 3. A heterozygous 2.40 Mb deletion at chromosome 11q13 in array-CGH analysis of Case 1
Source: Author

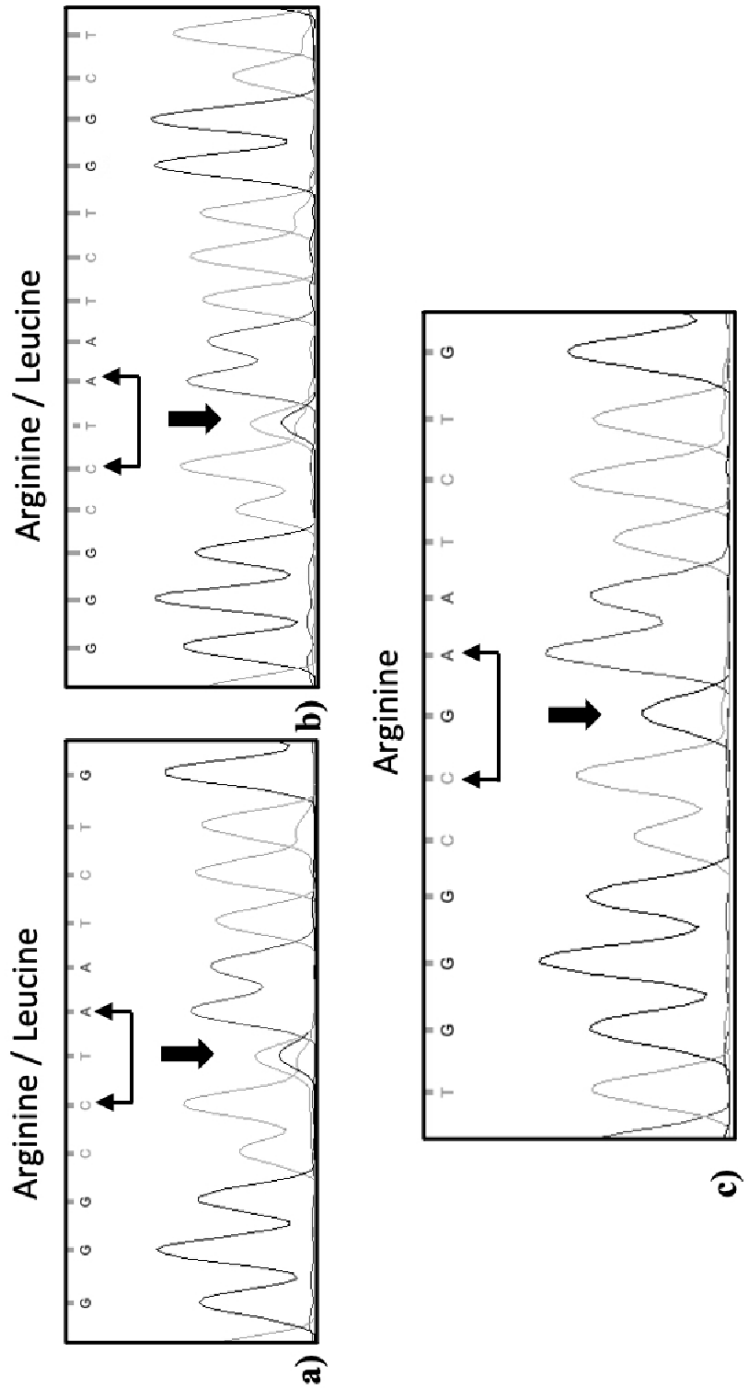

Fig. 4. a-b) Sequence analysis of heterozygous c.8T>G variation in exon 1 of FGF3 gene for mother and father of Case 2; c) Sequence analysis of homozygous c.8T>G variation in exon 1 of *FGF3* gene of Case 2
Source: Author

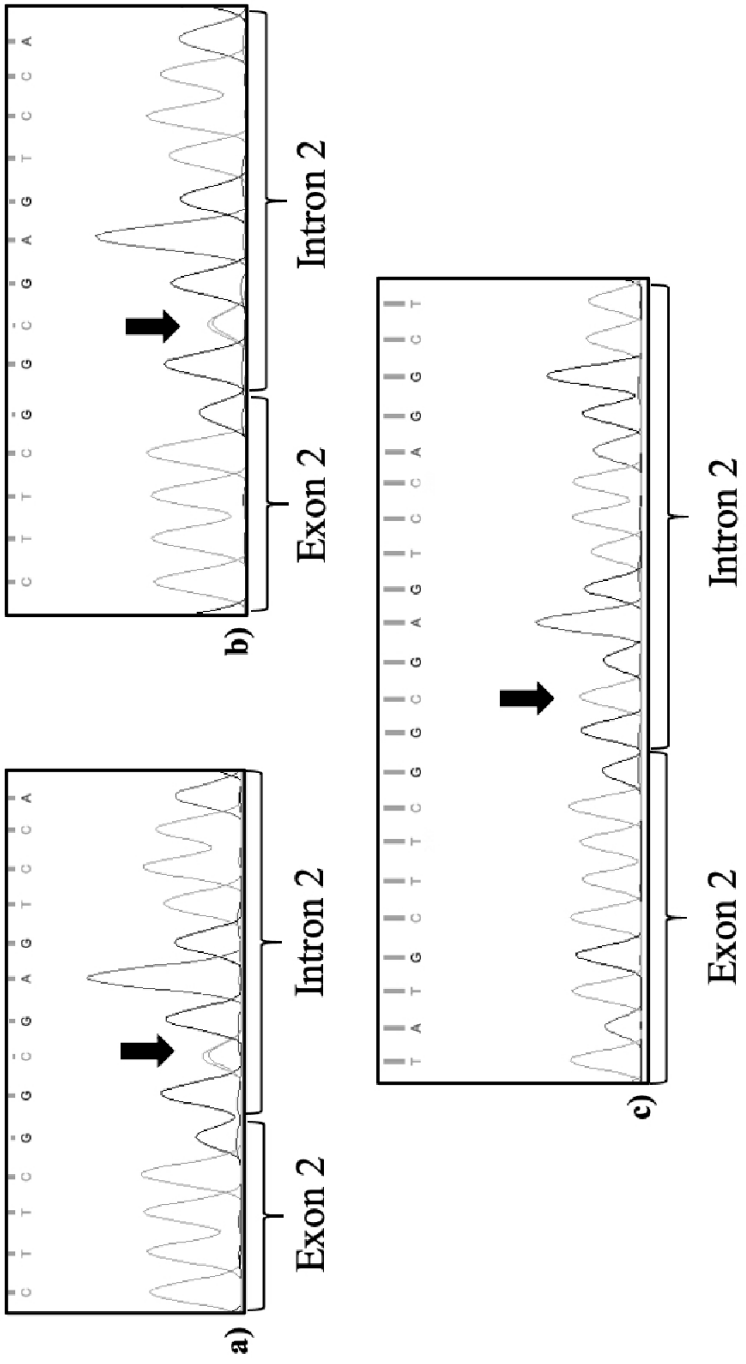

Fig. 5. a-b) DNA sequencing of heterozygous c.324 + 2T> C variation in intron 2 splice donor site of FGF3 gene for mother and father of Case 3; c) DNA sequence analysis of homozygous c.324+2T>C variation in intron 2 splice donor site of *FGF3* gene for Case 3
Source: Author

ies [such as 1000 Genome, genome aggregation database (gnomAD)]. *In silico* analysis (Mutation Taster, SIFT, DANN, FATHMM) predicted that it could be disease-causing. Segregation analysis showed that healthy parents carried the heterozygous variant (Fig. 4a-b). A novel homozygous splice-site variant (NM_005247: c.324+2T>C) was detected in case 3 (Fig. 5c). This variant was found to be heterozygous in gnomAD in one case, was never reported to be homozygous in the current databases and allele frequency was low (0.000003977). *In silico* analysis (Mutation Taster, HSF, DANN, FATHMM-MKL) predicted that this variant, which was not previously reported in the literature, may be disease-causing. According to the ACMG criteria, it was considered as pathogenic (Richards et al. 2015). Segregation analysis showed that healthy parents carried the heterozygous variant (Fig. 5a-b).

The clinical and molecular genetic results of all cases are summarized in Table 1.

DISCUSSION

The OMIM® database reveals that the FGF3 gene is associated with two different phenotypes. The first described phenotype is otodental dysplasia, which results from a contiguous gene deletion syndrome at chromosome 11q13, an area which includes the *FGF3* gene (OMIM: #166750). Otodental dysplasia is a disease characterized by facial dysmorphic manifestations, sensorineural hearing loss, and dental anomalies (globodontia, taurodontia, pulp stones and enamel defects) (Gregory-Evans et al. 2007). Later, Tekin et al. (2007) defined a phenotype that was described as displaying "congenital deafness, with inner ear agenesis, microtia, and microdontia" (OMIM: #610706). This phenotype, which later came to be known as LAMM syndrome, is characterized by facial dysmorphic manifestations, congenital sensorineural hearing loss, microtia, microdontia and neuromotor developmental retardation. Functional studies have shown that the *FGF3* gene is essential for normal development of the inner ear, teeth and auricula in the early embryonic period (Ornitz et al. 2001). Thus, when the patients carrying homozygous mutation in the *FGF3* gene were studied, varied effects were observed on the development of teeth, inner ears, and auricles, which

Table 1: Clinical, radiologic and genetic features of the patients

	Case 1	*Case 2*	*Case 3*
Age (year)	2	5	6
Sex	M	F	M
Consanguinity	-	+	+
Height (cm/SDS)	82 cm (-1.6 SDS)	113 cm (+ 0.85 SDS)	124.5 cm (+ 1.76 SDS)
Weight (kg/SDS)	9.5 kg (-2.47 SDS)	17 kg (-0.57 SDS)	24 kg (+ 1 SDS)
Head circumference (cm/SDS)	47 cm (-1.5 SDS)	50 cm (-0.48 SDS)	52 cm (+0.14 SDS)
Congenital hearing loss	+	+	+
External ear anomaly	Low-set and cupped shaped small ears, bilateral preauricular skin tags	Small cupped shaped ears, preauricular skin tag	Small cupped shaped ears, bilateral postauricular skin tags
MRI results of inner ear anomaly	Advanced hypoplasia in the left IAC, 7^{th}–8^{th} nerve complexes ext ending into the canal did not have normal appearance,	Michel's aplasia	Michel's aplasia
Dental anomaly	Small widely spaced teeth	Microdontia, small widely spaced teeth	Microdontia, small widely spaced teeth
Additional findings	Atrial septal defect, simian crease on the left hand	Neurodevelopmental delay, miyopia	Neurodevelopmental delay
Molecular analysis results	Heterozygous deletion of a 2.40 Mb segment in chromosome 11q13.3-q 13.4, including the *FGF3* gene	Homozygous c.8T>G, p.Leu3Arg	Homozygous c.324+2T>C

M: male, F: female, -: absence, +: presence, SDS: standart deviation score, MRI: : magnetic resonance imaging

support the presence of phenotypic variability in this gene mutation (Riazuddin et al. 2011).

There are approximately 43 cases of otodental dysplasia reported in the literature so far. In most of the cases, dental anomalies have been examined in detail, whereas hearing loss, and other anomalies have also been reported in some cases. The finding of facial dysmorphism in cases reported in this study are compatible with the known syndrome but differ from the cases in the literature with some additional anomalies. In case 1, at the age of 10 months, otodental dysplasia was diagnosed on the basis of congenital hearing loss, facial dysmorphic findings, and temporal bone MRI findings. However, in the literature indicates that sensorineural hearing loss occurs in early childhood, and the earliest case was diagnosed at the age of 4 years. In addition, all such cases reported normal cranial MRIs in the patients (Kim et al. 2016; Liu et al. 2017; Su et al. 2019). The researchers believe that the researchers' case differs from previously reported cases due to congenital hearing loss as well as the abnormalities found during cranial MRI. Furthermore, coloboma can occur in cases that involve *FADD* gene in the deleted region, but the researchers did not detect coloboma during a detailed eye examination of the researchers' case. However, the case was followed up by intermittent eye examination. In addition, while ASD was detected in case 1, congenital heart anomaly was not detected any of the cases described in the literature.

Till date, 69 cases of LAMM syndrome have been reported in the literature that involved 20 families. In 91 percent of the cases, there is consanguinity between the parents. Congenital sensorineural hearing loss and external ear anomaly were present in all cases. In case of external ear anomaly, 37 cases were affected symmetrically, and 32 cases were affected asymmetrically. In addition, 78 percent of the cases had type 1 microtia, while cup shape, simple, protruding ear, auricular skin tag, and shortened upper part auricular anomalies have been reported in the rest of the cases. Inner ear MRI revealed complete Michel's anomaly in 20 cases, while additional anomalies were found in the rest of the cases. Inner ear anomaly detected in this way was symmetrical in 28 cases and asymmetrical in 41 cases. Dental anomaly was found in all cases, and the most common was small widely spaced teeth anomaly (Tekin et al. 2007; Tekin et al. 2008; Ramsebner et al. 2010; Alsmadi et al. 2009; Riazuddin et al. 2011; Sensi et al. 2011; Schaefer et al. 2014; Singh et al. 2014; Basdemirci et al. 2019). Motor delay was detected in two cases reported by Al Yassin et al. and myopia was detected in one case reported by Basdemirci et al. (Al Yassin et al. 2019; Basdemirci et al. 2019). The researchers' cases (cases 2 and 3) were symmetrically affected in terms of external ear anomaly and both had a small cupped shaped ear. Interestingly, the postauricular skin tag found in case 3 had not been previously reported in the literature. In addition, dysmorphic findings such as narrow forehead, deep-set-eyes, down-slanting palpebral fissures, and depressed nasal bridge found in case 2 have not been reported in the literature either. The researchers detected Michel's anomaly in both the researchers' cases and they were affected symmetrically. In both cases, small widely spaced teeth as well as dental anomalies were detected, which aligns with previously published literature. Lastly, motor delay was detected in both cases, while myopia was also detected only in case 2.

The homozygous mutation the researchers detected in case 2 (NM_005247: c.8T>G, p. Leu3 Arg) was located in the region encoding 17-amino acid signal peptide in the N-terminus region of the FGF3 protein. This signal peptide is necessary to direct the corresponding protein, which comprises of 16–30 mostly hydrophobic amino acids, to the secretory pathway of the cell. In the researchers' case, the researchers predicted that the protein secretion would therefore be disrupted by the hydrophobic Leucine-to-Arginine substitution at codon 3. The p.Leu6Pro homozygous mutation detected by Tekin et al. (2008) in the three Turkish siblings with LAMM syndrome was based on a similar prediction that the signal peptide structure would be affected, thus resulting in an impaired protein secretion. Therefore, the mutation the researchers detected is the second known mutation which is projected to disrupt the function of the FGF3 protein signal peptide.

The homozygous c.324 + 2T> C mutation detected in case 3 was considered to be disease-causing because it was predicted that it would impair splicing according to ACMG criteria and *in-silico* analysis (Richards et al. 2015). The c.324+2T>C mutation is in splice donor site of intron 2 of the

FGF3 gene. Thus, this mutation may cause skipping of exon 2 which encodes the FGF domain of the FGF3 protein, and its loss can affect the function of this domain (Anna et al. 2019). If exon 2 is skipping, it leads to a shift in the open reading frame which results in stop codon at codon 92. These alterations can lead to truncated protein and/or nonsense mediated mRNA decay. However, functional studies could not be done at the protein level. This mutation is the first splice-site mutation defined in the *FGF3* gene.

CONCLUSION

In this study, the researchers present two cases of LAMM syndrome arising from two different families with typical clinical findings, and a case of otodental dysplasia with atypical clinical and radiological findings, both diagnosed at an early stage. All three cases described in this study expand the phenotypic features known to be associated with otodental dysplasia and the LAMM syndrome. In addition, our understanding of the molecular etiology of the disease has been enhanced by the discovery of novel genetic variants of the LAMM syndrome.

RECOMMENDATIONS

In case of absence of inner ear structures in patients that report syndromic hearing loss, *FGF3* gene related phenotypes should be considered. Moreover, *FGF3* gene should be examined by sequence analysis and array-CGH methods for both point mutations and gross deletions to better understand the etiology of associated disease.

REFERENCES

Al Yassin A, D'Arco F, Morín M et al. 2019. Three new mutations and mild, asymmetrical phenotype in the highly distinctive LAMM Syndrome: A report of eight further cases. *Genes,* 10(7): 529.

Alsmadi O, Meyer BF, Alkuraya F et al. 2009. Syndromic congenital sensorineural deafness, microtia and microdontia resulting from a novel homoallelic mutation in fibroblast growth factor 3 (FGF3). *Eur J Hum Genet,* 17(1): 14-21.

Alvarez Y, Alonso MT, Vendrell V et al. 2003. Requirements for FGF3 and FGF10 during inner ear formation. *Development,* 130: 6329–6338.

Anderson MJ, Schimmang T, Lewandoski M 2016. An FGF3-BMP signaling axis regulates caudal neural tube closure, neural crest specification and anterior-posterior axis extension. *PLoS Genet,* 12(5): e1006018.

Anna A, Monika G 2019. Splicing mutations in human genetic disorders: Examples, detection, and confirmation [published correction appears in J Appl Genet, 60(2): 231]. *J Appl Genet,* 59(3): 253-268.

Anwar T, Rufail ML, Djomehri SI et al. 2020. Next-generation sequencing identifies recurrent copy number variations in invasive breast carcinomas from Ghana. *Mod Pathol,* 33(8): 1537-1545.

Basdemirci M, Zamani AG, Sener S et al. 2019. LAMM syndrome: Two new patients with a novel mutation in FGF3 gene and additional clinical findings. *Clin Dysmorphol,* 28(2): 81-85.

Brown J, Stepien AJ, Willem P 2020. Landscape of copy number aberrations in esophageal squamous cell carcinoma from a high endemic region of South Africa. *BMC Cancer,* 20(1): 281.

Carpio Horta K, Weiss SG, Miranda K et al. 2019. Polymorphisms in FGF3, FGF10, and FGF13 may contribute to the presence of Temporomandibular Disorders in patients who required orthognathic surgery. *J Craniofac Surg,* 30(7): 2082-2084.

Chung JH, Dewal N, Sokol E et al. 2019. Prospective comprehensive genomic profiling of primary and metastatic prostate tumors. *JCO Precis Oncol,* 3: 10.1200/PO.18.00283.

Cunha AS, Dos Santos LV, Marañón-Vásquez GA et al. 2020. Genetic variants in tooth agenesis-related genes might be also involved in tooth size variations [published online ahead of print, 2020 Jul 9]. *Clin Oral Investig,* 10.1007/s00784-020-03437-8.

Gregory-Evans CY, Moosajee M, Hodges MD et al. 2007. SNP genome scanning localizes auto-dental syndrome to chromosome 11q13 and microdeletions at this locus implicate FGF3 in dental and inner-ear disease and FADD in ocular coloboma. *Hum Mol Genet,* 16(20): 2482 2493.

Hatch EP, Noyes CA, Wang X et al. 2007. Fgf3 is required for dorsal patterning and morphogenesis of the inner ear epithelium. *Development,* 134: 3615–3625.

Kim YS, Kim GH, Byeon JH et al. 2016. Chromosome 11q13 deletion syndrome. *Korean J Pediatrics,* 59 (Suppl 1): S10-S13.

Küchler EC, Lips A, Tannure PN et al. 2013. Tooth agenesis association with self-reported family history of cancer. *J Dent Res,* 92(2): 149-155.

Li YF, Hsiao YH, Lai YH et al. 2015. DNA methylation profiles and biomarkers of oral squamous cell carcinoma. *Epigenetics,* 10(3): 229-236.

Liu A, Wu M, Guo X et al. 2017. Clinical, pathological, and genetic evaluations of Chinese patient with otodental syndrome and multiple complex odontoma: Case report. *Medicine,* 96(5): e6014.

Mansour SL, Goddard JM, Capecchi MR 1993. Mice homozygous for a targeted disruption of the protooncogene int-2 have developmental defects in the tail and inner ear. *Development,* 117: 13–28.

Motta Gda R, Amaral MV, Rezende E et al. 2014. Evidence of genetic variations associated with rotator

cuff disease. *J Shoulder Elbow Surg,* 23(2): 227-235.
Ornitz DM, Itoh N 2001. Fibroblast growth factors. *Genome Biol,* 2: 3005.1–3005.12.
Pauley S, Wright TJ, Pirvola U et al. 2003 Expression and function of FGF10 in mammalian inner ear development. *Giant Dyn,* 227: 203-215.
Ramsebner R, Ludwig M, Parzefall T et al. 2010. A FGF3 mutation associated with differential inner ear malformation, microtia, and microdontia. *Laryngoscope,* 120(2): 359-364.
Riazuddin S, Ahmed ZM, Hegde RS et al. 2011. Variable expressivity of FGF3 mutations associated with deafness and LAMM syndrome. *BMC Med Genet,* 12: 21.
Richards S, Aziz N, Bale S et al. 2015. Standards and guidelines for the interpretation of sequence variants: A joint consensus recommendation of the American College of Medical Genetics and Genomics and the Association for Molecular Pathology. *Genet Med,* 17: 405-424.
Rohmann E, Brunner HG, Kayserili H et al. 2006. Mutations in different components of FGF signaling in LADD syndrome. *Nature Genet,* 38: 414–417.
Schaefer E, Minoux M, Lauer J et al. 2014. A novel mutation involving the initiation codon of FGF3 in a family described with complete inner ear agenesis, microtia and major microdontia (LAMM syndrome). *J Genet Syndr Gene Ther,* 5: 1–5.
Sensi A, Ceruti S, Trevisi P et al. 2011. LAMM syndrome with middle ear dysplasia associated with compound heterozygosity for FGF3 mutations. *Am J Med Genet A,* 155A(5): 1096-1101.
Singh A, Tekin M, Falcone M et al. 2014. Delayed presentation of rickets in a child with labyrinthine aplasia, microtia and microdontia (LAMM) syndrome. *Indian Pediatr,* 51(11): 919-920.
Su JM, Zeng SJ, Ye XW et al. 2019. Three years of follow-up of autodental syndrome in 3-year-old Chinese boy: A rare case report. *BMC Oral Health,* 19(1): 164.
Tekin M, Hiºmi BO, Fitoz et al. 2007. Homozygous mutations in fibroblast growth factor 3 are associated with a new form of syndromic deafness characterized by inner ear agenesis, microtia, and microdontia. *Am J Hum Genet,* 80(2): 338-344.
Tekin M, Oztürkmen Akay H, Fitoz S et al. 2008. Homozygous FGF 3 mutations result in congenital deafness with inner ear agenesis, microtia, and microdontia. *Clin Genet,* 73(6): 554-565.
Wright TJ, Mansour SL 2003. Fgf3 and Fgf10 are required for mouse otic placode induction. *Development,* 130: 3379–3390.

Paper received for publication in June, 2020
Paper accepted for publication in August, 2020